Received: 23 December 2025 | Accepted: 8 May 2026

DOI: 10.1002/hem3.70405

HemaSphere eha

ARTICLE

Minimally invasive characterization of peripheral blood measurable residual disease in multiple myeloma using high-sensitivity detection of ctDNA by next-generation sequencing

Natalia Buenache[1] | Marta Lasa[2] | Andrés Arroyo[1] | Carmen González[2] | Larissa Haertle[1,3,4] | Yanira Ruiz-Heredia[1] | Rosa Ayala[1] | Rafael Alonso[1] | Alejandro Martín-Muñoz[5] | Juan M. Rosa-Rosa[1] | Verónica González[6] | María J. Calasanz[2] | Paula Rodríguez-Otero[2] | Laura Rosiñol[7] | Felipe De Arriba[8] | Enrique M. Ocio[9] | Albert Oriol[10] | Yolanda González[11] | Anna Sureda[12] | Sunil Lakhwani[13] | María E. Clavero[14] | Angela Ibáñez[15] | Clara Gómez[16] | Alberto Orfao[6] | María-Victoria Mateos[6] | Juan J. Lahuerta[1] | María T. Cedena[1] | Joan Bladé[7] | Jesús San Miguel[2] | Noemi Puig[6] | Bruno Paiva[2] | Joaquín Martínez-López[1]

Graphical Abstract

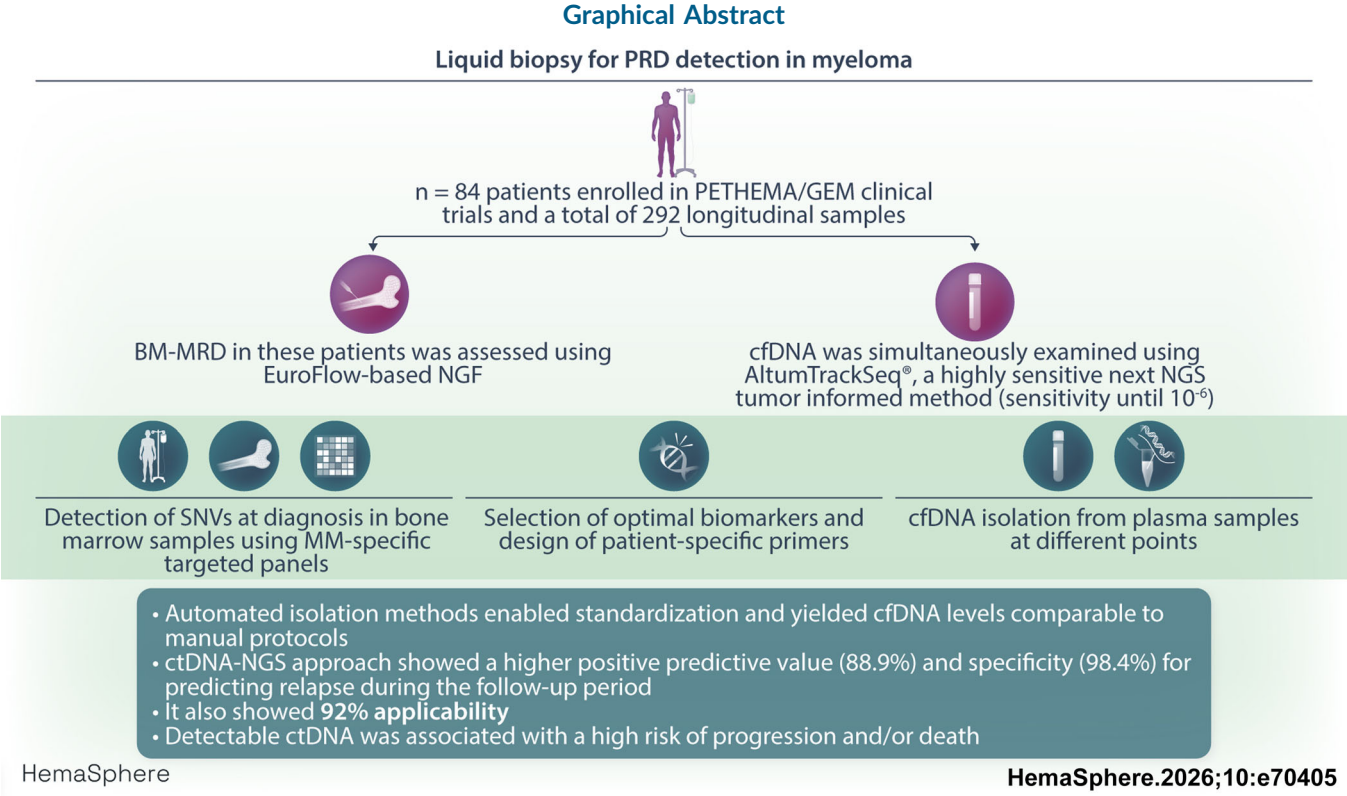

Received: 23 December 2025 | Accepted: 8 May 2026

DOI: 10.1002/hem3.70405

ARTICLE

HemaSphere eha

Minimally invasive characterization of peripheral blood measurable residual disease in multiple myeloma using high-sensitivity detection of ctDNA by next-generation sequencing

Natalia Buenache[1] | Marta Lasa[2] | Andrés Arroyo[1] | Carmen González[2] | Larissa Haertle[1,3,4] | Yanira Ruiz-Heredia[1] | Rosa Ayala[1] | Rafael Alonso[1] | Alejandro Martín-Muñoz[5] | Juan M. Rosa-Rosa[1] | Verónica González[6] | María J. Calasanz[2] | Paula Rodríguez-Otero[2] | Laura Rosiñol[7] | Felipe De Arriba[8] | Enrique M. Ocio[9] | Albert Oriol[10] | Yolanda González[11] | Anna Sureda[12] | Sunil Lakhwani[13] | María E. Clavero[14] | Angela Ibáñez[15] | Clara Gómez[16] | Alberto Orfao[6] | María-Victoria Mateos[6] | Juan J. Lahuerta[1] | María T. Cedena[1] | Joan Bladé[7] | Jesús San Miguel[2] | Noemi Puig[6] | Bruno Paiva[2] | Joaquín Martínez-López[1]

Correspondence: Joaquín Martínez-López (jmarti01@ucm.es)

Abstract

Measurable residual disease assessment in bone marrow (BM-MRD) is a crucial prognostic factor in multiple myeloma (MM), but its clinical use has some caveats, such as invasiveness, poor spatial representativity, and serial sampling. Novel minimally invasive approaches for monitoring peripheral residual disease (PRD) could facilitate its clinical use. We aimed to investigate a sensitive method for detecting PRD in patients with MM. This study included 84 patients enrolled in PETHEMA/GEM clinical trials, and a total of 292 longitudinal samples were analyzed. BM-MRD in these patients was assessed using EuroFlow-based next-generation flow cytometry (NGF) and PRD was simultaneously examined in cell-free DNA (cfDNA) using AltumTrackSeq®, a highly sensitive next-generation sequencing (NGS) method based on patient-specific multiplexed amplicon mini-panels that target somatic mutations identified at diagnosis. Our findings revealed that automated isolation methods enabled standardization and yielded cfDNA levels comparable to manual protocols. A high median cfDNA concentration of 393.2 ng was obtained, with a range from 17.3 to 6300 ng. Furthermore, we demonstrated that compared with traditional BM-MRD by NGF, our ctDNA-NGS approach showed a higher positive predictive value (PPV, 88.9% vs. 34.5%) and specificity (Sp, 98.4% vs. 70.3%) for predicting relapse during the follow-up period. Detectable ctDNA was associated with a high risk of progression and/or death (HR, 11.5; 95% CI, 2.66–49.4), and this was confirmed in the multivariate analysis. In conclusion, this assay offers a method for detecting imminent relapse risk in the peripheral blood of MM patients.

[1]Hematological Malignancies Clinical Research Unit, Hospital Universitario 12 de Octubre, Universidad Complutense, Madrid, Spain
[2]Cancer Center Clinica Universidad de Navarra, Centro de Investigación Médica Aplicada (CIMA), Instituto de Investigacion Sanitaria de Navarra (IDISNA), Universidad de Navarra, Pamplona, Spain
[3]Department of Medicine III, Technical University of Munich, School of Medicine and Health, TUM University Hospital, Munich, Germany
[4]TranslaTUM, Center for Translational Cancer Research, Technical University of Munich, Munich, Germany
[5]Altum Sequencing Co., Madrid, Spain

INTRODUCTION

In multiple myeloma (MM), bone marrow measurable residual disease (BM-MRD) has emerged as a crucial indicator for assessing patient response to treatment.[1–3] Despite advancements in therapies necessitating frequent assessments for disease monitoring, the irregular bone marrow infiltration characteristic of MM presents challenges for effective follow-up. Likewise, BM-MRD assessment can be compromised by the focal nature of the disease. Despite the presence of disease in the bone marrow, it may not be fully represented at the biopsy site, resulting in false-negative results even with high sensitivity (Se) (up to 10^{-6}), particularly in cases with plasmacytomas, where disease localization can lead to incomplete sampling.[4]

Emerging liquid biopsy approaches for peripheral residual disease (PRD) and circulating biomarker detection hold promise for improving response assessment in MM. These approaches include detection of circulating tumor cells (CTCs), use of mass spectrometry to identify low levels of M-protein, and analysis of circulating tumor DNA (ctDNA). While detecting CTCs in MM poses challenges due to the typically lower tumor cell burden in peripheral blood (PB) compared to the BM, often by two orders of magnitude,[5] advancements in highly sensitive detection technologies are helping to overcome this limitation. Similarly, although mass spectrometry-based methods for detecting M-protein can be unreliable due to the persistence of low immunoglobulin levels in serum—due to the long half-life and not necessarily persistent residual disease—potentially leading to false-positive results, ongoing refinements are enhancing their specificity (Sp) and clinical utility.[5] Cell-free DNA (cfDNA) is released into the bloodstream by both malignant and nonmalignant cells, with plasma concentrations varying according to physiological and pathological conditions. Notably, elevated cfDNA levels have been consistently observed in patients with malignant neoplasms.[6–8] Consequently, cfDNA has been explored as a potential biomarker for cancer detection; however, only the tumor-specific fraction, ctDNA, offers the requisite Se and Sp for reliable cancer detection applications.[9] This detection of ctDNA may also provide insights into tumor biology. Nevertheless, current ctDNA detection technologies face limitations, struggling to achieve sensitivities greater than 10^{-4} in PB.[10] Typically, 30 ng of cfDNA contains the genomic material of approximately 10,000 cells. Increasing Se is challenging due to the limited volume of blood that can be drawn (usually 20 mL). One way to improve Se is by analyzing a larger panel of biomarkers, and tandem single-nucleotide variant sequencing (tSNV-Seq) detection has been shown to increase Se by one order of magnitude in lymphoid neoplasm.[11,12] In the present study, we aimed to develop a high-Se tumor-informed method for detecting ctDNA in patients with MM by using large plasma volumes and identifying tandem variants. Subsequently, we assessed the clinical significance of PRD monitoring using next-generation sequencing (NGS) in identifying patients with different treatment outcomes.

MATERIALS AND METHODS

Study design

This ad hoc study involved 84 newly diagnosed patients with MM who were either on maintenance therapy or under observation, within the PETHEMA/GEM clinical trial framework, at the point of MRD assessment. Specifically, 65 of these patients were from the GEM2017FIT clinical trial, and 19 patients were enrolled in other trials. The principal characteristics of the patients are summarized in Table 1.

The main criteria for including patients in this study were the availability of sufficient plasma from sequential samples and existing baseline genotyping information at diagnosis. All patients with ctDNA-positive samples in this study were in serological and clinical complete response at the time of their ctDNA-positive detection. In all the patients included in this study by protocol, BM aspirates were prespecified to be collected every year during maintenance and observation during a period of 5 years after consolidation. PB samples were pre-specified to be collected every 6 months after consolidation. MRD was assessed using next-generation flow cytometry (NGF) on BM aspirate samples collected at various follow-up time points for each patient, according to the clinical trial procedures. In parallel, 292 PB samples were analyzed using AltumTrackSeq® (Altum sequencing), a tumor-informed MRD test based on ctDNA detection by NGS.[13,14] Briefly, at each time point, a large volume (50 mL) of blood was collected in EDTA tubes and processed within 24 h. Following centrifugation, the samples were divided into two plasma aliquots, which were then frozen at −80°C until further use. One of these large-volume plasma aliquots was collected in Falcon® collection tubes (Corning), after which cfDNA purification was performed. Somatic mutations identified in these baseline samples served as disease biomarkers for PRD-NGS analysis at subsequent follow-up time points.

cfDNA isolation methods

Initially, we evaluated several methods for processing cfDNA for PRD-NGS analysis to identify the most efficient approach based on available laboratory resources and reagents. All strategies were equally capable of cfDNA extraction, ensuring that the selection of methodology presumably did not impact the results or their reliability. We then quantified the cfDNA concentration using both manual and (semi-)automated methods with varying elution volumes. The manual method, the QIAamp Circulating Nucleic Acid (QCNA) Kit (Qiagen), a silica membrane-based isolation technique, was used for cfDNA extraction in 69 of the 292 plasma samples. The Maxwell® RSC LV ccfDNA Kit (RSC) (Promega), a semi-automated method utilizing paramagnetic beads, was applied to 22 samples. These samples were subjected to manual preprocessing with a rotary mixer to enhance circulating cell-free DNA (ccfDNA) purification from human plasma.

[6]Hospital Universitario de Salamanca, Instituto de Investigación Biomédica de Salamanca, Salamanca (IBSAL), Universidad de Salamanca, Salamanca, Spain
[7]Amyloidosis and Myeloma Unit, Department of Hematology, IDIBAPS, Hospital Clínic de Barcelona, Barcelona, Spain
[8]Servicio de Hematología. Hospital General Universitario Morales Meseguer. Instituto Murciano de Investigación Biosanitaria (IMIB-Pascual Parrilla), Universidad de Murcia, Murcia, Spain
[9]Hospital Universitario Marqués de Valdecilla (IDIVAL), Universidad de Cantabria, Santander, Spain
[10]Institut Català d'Oncologia i Institut Josep Carreras, Hospital Germans Trias i Pujol, Badalona, Barcelona, Spain
[11]Institut d'Oncologia Dr. Josep Trueta, Girona, Spain
[12]Institut Català D'Oncologia, Hospital Duran i Reynals, Institut d'Investigacio Biomedica de Bellvitge (IDIBELL), Universitat de Barcelona, Barcelona, Spain
[13]Hospital Universitario de Canarias, Santa Cruz de Tenerife, Spain
[14]Hospital Virgen de las Nieves, Granada, Spain
[15]Complejo Hospitalario Universitario de Albacete, Albacete, Spain
[16]Hospital Universitario de Galdakao, Vizcaya, Spain

TABLE 1 Demographics, treatment, and depth of response in the 77 patients included in the final study cohort.

	All patients (*N* = 77)	NGS PRD negative (*N* = 68)	NGS PRD-positive (*N* = 9)	P-value
Gender, *n* (%)				
Male	35	33 (48.5%)	3 (33,3%)	0.5
Female	42	35 (51.5%)	6 (66.7%)	
Age, median (range)	77	71 (67–74)	68 (65–71)	0.4
Treatment arm, *n* (%)				
K-based	27	23 (33.9%)	4 (44.5%)	>0.9
K-Dara-based	23	21 (30.9%)	2 (22.2%)	
VR-based	27	24 (35.2%)	3 (33.3%)	
R-ISS, *n* (%)				
I	23	22 (32.4%)	1 (11.1%)	0.4
II	44	37 (54.4%)	7 (77.8%)	
III	10	9 (13.2%)	1 (11.1%)	
Cytogenetic, *n* (%)				
Standard risk	47	43 (63.2%)	4 (44.4%)	0.5
High risk	17	14 (20.6%)	3 (33.4%)	
Not available	13	11 (16.2%)	2 (22.2%)	

Abbreviations: Dara, daratumumab; K, carfilzomib; NGS, next-generation sequencing; PRD, peripheral residual disease; R-ISS, Revised International Staging System; VR, bortezomib plus lenalidomide.

Finally, the entirely automated EZ1&2 ccfDNA (EZ1) Kit (Qiagen), which also uses magnetic bead technology, was used to purify cfDNA from the remaining 201 plasma samples. All extracted cfDNA samples were quantified using a Qubit HS Kit (Thermo Fisher Scientific). Notably, over 300 ng of cfDNA was obtained in 18% of the samples, more than 100 ng from 55% of the samples, and more than 30 ng from 92% of the samples.

Dual size-selection purification

Fragment size and genomic DNA (gDNA) contamination were quantified using a Bioanalyzer 2100 fragment analysis system (Agilent). Samples with a cfDNA/gDNA ratio below 1 were subjected to purification to remove gDNA (Additional File 1, Figure S1). Subsequently, cfDNA samples were purified and size-selected using AMPure XP magnetic beads (Beckman Coulter Life Sciences). This size selection was performed by adapting the protocol described by Chauhan and colleagues,[15] using a two-step bead-based selection with a first bead-to-sample ratio of 0.6× to exclude high-molecular-weight DNA, followed by a second ratio of 1.8X to retain fragments within the target size range (150–200 bp).

Baseline genotyping and PRD biomarker selection

Baseline genotyping was conducted on CD138+ plasma cells collected from BM samples from each of the 84 patients at screening using a customized gene panel designed for MM[16] or a commercially available equivalent. This analysis was performed if sufficient genetic material was available using the customized panel (in 25 patients) or could be inferred from tumor data provided by the referring hospital for the remaining 59 patients. Once all mutations were identified, the optimal PRD-NGS biomarkers were selected for each patient through a multi-step process. First, all potential single-nucleotide polymorphisms (SNPs), germline variants and variants of uncertain significance (VUS) that could compromise result reliability were filtered out using the COSMIC, CLinVar, and dbSNP databases.[13] The remaining somatic mutations were then categorized, and those most frequently associated with MM were prioritized. The goal was to identify 5–10 informative markers per patient whenever feasible.

Tumor-informed ctDNA profiling using the AltumTrackSeq® technology

From initial PB volumes ranging from 2 to 32 mL, the mean total amount of cfDNA considering the final state of the samples, whether processed through purification or not, was 211.36 ng (range 7.5–2527.2 ng). Samples were excluded due to residual gDNA contamination, as determined by electropherogram analysis, when the cfDNA/gDNA ratio was <1 despite dual size-selection purification. The minimum targeted amount of cfDNA for sequencing was 30 ng. Given that one haploid genome equivalent (hGE) has a mass of ~3 pg,[17] 30 ng of cfDNA is sufficient to screen 10,000 hGEs, achieving a theoretical limit of detection (LoD) with a Se of at least 10^{-4}. This Se could be further improved to 1.4×10^{-5} variant allele frequency (VAF) (0.0014%) with the mean input of cfDNA in our assay and to a maximum Se of 1.2×10^{-6} VAF (0.000 12%) when 2500 ng of cfDNA was used. In total, 12 samples (4%) were not evaluable due to unsatisfactory sequencing performance, and a further 22 samples (8%) were excluded because they yielded <30 ng of cfDNA. Finally, we established the limit of detection (LoD) for each mutation by analyzing normal controls, applying a stringent threshold of $10^{-}4$.

ctDNA was obtained from plasma samples collected at various follow-up time points and processed according to the criteria established above. These ctDNA samples were then analyzed using the AltumTrackSeq® technology. This highly sensitive NGS approach used patient-specific amplicon-multiplexed mini-panels designed to target somatic mutations identified at diagnosis. Each mini-panel utilized molecularly tagged primer pairs (6-mer tags) to amplify these mutations in three biological replicates (P1, P2, and P3), allowing the exclusion of data that show significant deviation. The tagged post-PCR products were pooled for library preparation and subsequently sequenced on the Ion S5 System platform (Life Technologies, Thermo Fisher Scientific Inc.), achieving a sequencing depth of 500,000× per amplicon, as previously described.[18,19] Following sequencing, a bioinformatic pipeline implemented in Python and R was used to filter out low-quality reads. For each mutation, the corrected VAF was compared to its LoD, and mutations falling below the threshold were excluded from further analysis. MRD status was determined by identifying the mutation with the highest VAF at each follow-up time point. Samples with VAFs above the established Se limit were classified as MRD-positive, while those below this threshold were designated as MRD-negative.[13]

Detection of tandem variants

Tandem single-nucleotide variant sequencing (tSNV-Seq) was also integrated into the AltumTrackSeq® test to further increase ctDNA detection Se. These genetic markers, consisting of multiple somatic mutations or tandem variants within 100 bp of the same DNA strand or fragment, provide a 10- to 100-fold higher Se than other genetic

variants, such as SNVs, as detailed in Additional File 2, Figure S2. We identified these tandem variants at baseline samples by tSNV-Seq in 36% of the patients with our targeted panel.

Next-generation flow determination in the bone marrow

MRD in BM was assessed by NGF simultaneously with PRD-NGS. Follow-up samples were processed within 24 h of collection. Analysis was performed using the recently developed NGF methodology, in accordance with EuroFlow guidelines, as described in previous publications.[3,20–22] Data from two eight-color cytometry tubes per sample were merged using INFINICYT™ v2.0 software (Cytognos S.L.). A sample was considered positive if at least 20 aberrant plasma cells were detected.

Statistics

Patient and disease characteristics were summarized using descriptive statistics. Continuous variables were compared using the Wilcoxon rank-sum test for two-group comparisons and the Kruskal–Wallis test for comparisons involving more than two groups. Categorical variables were compared using Fisher's exact test where appropriate. The linear relationship between continuous variables was evaluated using Pearson's correlation coefficient.

The prognostic performance of both PRD-NGS and BM-MRD by NGF in predicting clinical relapse was evaluated by calculating the Se, Sp, positive predictive value (PPV), and negative predictive value (NPV). Clinical relapse occurring at any time during follow-up was used as the reference outcome. These metrics were derived from 2 × 2 contingency tables comparing MRD status (positive vs. negative) with relapse occurrence.

Progression-free survival (PFS) was defined, using a landmark approach, as the time from the first MRD assessment (MRD1) to documented disease progression or death. Patients without these events were censored at their last follow-up. To investigate the impact of clinical variables and MRD dynamics on PFS, time-dependent univariate and multivariate Cox proportional hazards models were applied. These models accounted for changes in MRD status over time, enabling a dynamic evaluation of its prognostic significance. Both PRD-NGS and BM-MRD by NGF were modeled as time-dependent covariates, with the data set structured to reflect exact time intervals between successive MRD assessments. Each observation interval was defined by the time elapsed between two consecutive MRD evaluations, allowing dynamic integration of longitudinal MRD status. Only patients and samples meeting predefined quality criteria were included. To ensure temporal consistency between the two MRD detection methods, analyses were restricted to intervals in which paired PRD-NGS and BM-MRD by NGF results were available from the same sampling date. We explored the association with PFS of clinically relevant baseline covariates such as age at MRD1, gender, induction treatment arm, Revised International Staging System (R-ISS), and cytogenetic risk sequentially adjusted for PRD-NGS and BM-MRD in separate bivariate analysis. Adjusted hazard ratios and 95% confidence intervals were estimated in a final multivariate model that included covariates with a bivariate $P < 0.2$.

Survival probabilities were estimated using Kaplan–Meier curves, and differences between groups were tested using the log-rank test. Patients were classified as MRD-positive if they had a positive MRD result at any time point and as MRD-negative if all their MRD assessments were undetectable throughout follow-up. The outcomes were defined according to the 2016 IMWG criteria.

All statistical analyses were performed using IBM SPSS Statistics version 22.0 (IBM Corp.) and R version 4.4.3 (R Foundation for Statistical Computing). GraphPad Prism version 8.01 (GraphPad Software) and R were used for data visualization. A two-sided $P < 0.05$ was considered statistically significant.

RESULTS

cfDNA extraction and optimization

The concentration of cfDNA was determined in a total of 292 plasma samples. These samples were processed using manual extraction with QCNA and two semi-automated methods: RSC and EZ1. From various volumes of plasma collected, quantification of total cfDNA prior to any purification steps revealed high yields in MM patient samples, with a median of 393.2 ng, ranging from 17.3 to 6300 ng. The mean total DNA yield from plasma samples was 567 ng (IQR: 189–790) and 474 ng (IQR: 143–653) for EZ1 and RSC, respectively ($P = 0.556$). By contrast, the QCNA method yielded a significantly higher DNA yield (mean 1099 ng; IQR: 289–1030) with statistically significant differences compared to the other methods ($P < 0.001$), suggesting a method-dependent variability in cfDNA recovery prior to purification (Figure 1A).

We next assessed the effect of increasing plasma volume on initial cfDNA recovery. We conducted the same analyses based on the initial plasma volume, which ranged from 2 to 32 mL (median: 8 mL), and the cfDNA isolation method (Additional File 3, Table S1). The data revealed significant increases in cfDNA recovery directly related to increasing plasma volume, with a clear escalation in DNA yield and notably high concentrations overall as well, from mean concentrations of 6.05 ng/μL (or a median of total cfDNA of 292 ng) for <10 mL, 11.72 ng/μL (or 628 ng) for 10–20 mL, and 22.88 ng/μL (or 1457 ng) for >20 mL group ($P < 0.001$) (Figure 1B).

Gel electrophoresis analysis of DNA integrity revealed a peak of longer fragments, indicating contaminating gDNA in 58% (168/292) of the cfDNA samples (Additional File 1, Figure S1), which can significantly dilute the tumor-derived ctDNA signal, but there was no relationship with initial plasma volume. Notably, the manual QCNA method showed the highest number of samples with a cfDNA/gDNA ratio <1, suggesting a greater amount of contaminating gDNA (50/69 samples). Although triplicate extractions could not be performed due to the high value of the clinical samples, the automatic EZ1 method, while yielding slightly less total DNA compared to QCNA, required fewer samples to be purified (108/201) ($P < 0.015$), with the additional observation of improved process standardization and suitability for high-throughput workflows. Regardless of the cfDNA extraction method, significant differences were observed between purified samples (168/292), with a median of 2.33 ng/μL (or 84 ng), and those that did not require a prior purification step with size selection (123/292), with a median of 5.14 ng/μL (or 257 ng) ($P < 0.001$) (Figure 1C). However, purification with dual size selection proved highly effective, removing contaminating gDNA in 98% of the samples (164/168). Following this purification step, the differences in cfDNA isolation methods were no longer statistically significant ($P = 0.56$) (Figure 1D). Furthermore, in 3.4% of samples requiring purification (6/174), the procedure could not be performed due to insufficient genetic material. Accordingly, the EZ1 method demonstrated greater efficiency, automation, and suitability for standardization compared to alternative approaches, supporting its selection for subsequent testing.

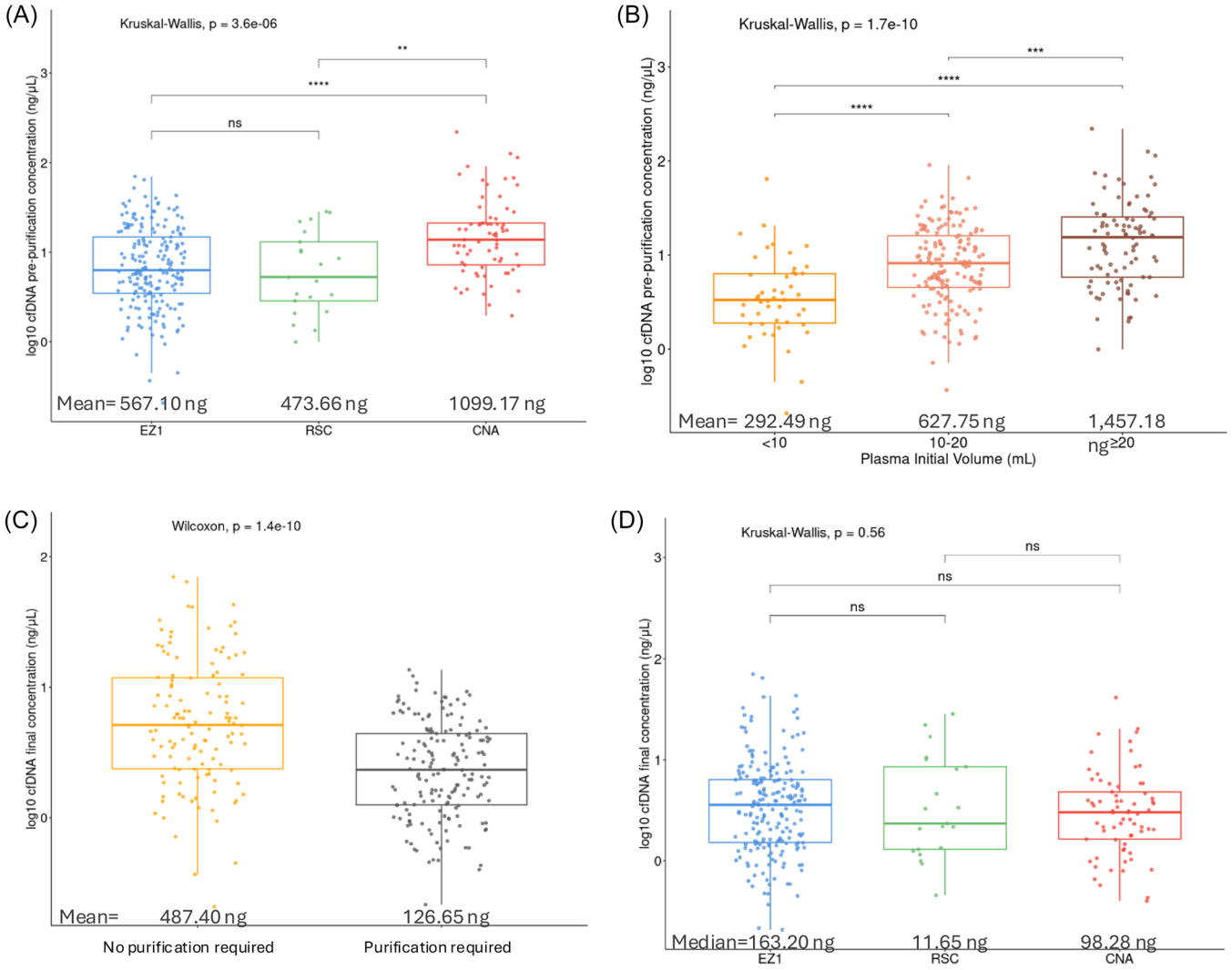

FIGURE 1 **Comparison of plasma cfDNA yield in MM patients across extraction methods and varying input volumes. (A)** Total DNA recovered per microliter of plasma using the EZ1 (n = 201), RSC (n = 22), and CNA (n = 69). **(B)** Correlation between cfDNA concentration and input plasma volume. **(C)** Samples requiring a prior purification step for gDNA removal. **(D)** Impact of postpurification on cfDNA yield. CNA, QIAamp Circulating Nucleic Acid; EZ1, EZ1&2 ccfDNA; ns, not significant; RSC, Maxwell RSC LV ccfDNA; log10 cfDNA <0: conc. <1 ng/µL; log10 cfDNA 0–1: 1–10 ng/µL; log10 cfDNA 1–2: 10–100 ng/µL; and log10 cfDNA 2–3: 100–1000 ng/µL. MM, multiple myeloma.

ctDNA detection

Baseline genotyping of the initial 84 patients with MM at diagnosis, using our customized gene panel or the commercial panel, identified a total of 150 somatic mutations (43 different genes), with a mean of 2.2 mutations per patient (median: 2; range: 1–6). These mutations, with a mean VAF of 0.289 (range: 0.01–0.831), were selected as potential biomarkers of PRD. The distribution of VAFs, including values < 0.03, was consistent with the presence of subclonal variants. The most frequently mutated genes were *KRAS* (25%), *NRAS* (16%), *ZFHX4* (7%), *DIS3* (6%), *FAT3* (6%), *FGFR3* (5%), *TP53* (5%), *TENT5C* (5%), *TRAF3* (4%), *BRAF* (4%), *ACTG1* (4%), *ATM* (3%), and *ZNF292* (3%). KRAS p.Gln61His and NRAS p.Gln61Arg mutations showed the highest incidence, found in 10/84 (11.9%) and 6/84 (7.1%) of patients, respectively. Suitable mutations for PRD monitoring were identified in 77 of the 84 patients (92% applicability). Potential germline variants or possible SNPs were identified in 7 of the remaining 84 patients (8%), and they were excluded from further ctDNA analysis. A total of 25 out of the 317 initially isolated cfDNA samples were obtained, resulting in a final data set of 292 samples eligible for downstream analysis.

In the follow-up analysis of 292 samples from the final 77 patients, our high-Se NGS approach detected ctDNA in 16 samples (5.5%) from 9 patients (12%), thus being positive for PRD-NGS. Among these PRD-positive samples, we identified 15 different mutations, with a mean of 1.56 mutations per patient (range: 1–3) and a mean VAF of 0.0077 (range: 1.25×10^{-4} – 1.03×10^{-1}). In patients with detectable ctDNA, the concentrations ranged from 125 to 8466 parts per million (PPM) (Additional Files 4-7, Figure S3-5 and Table S2).

For patients with undetectable MRD in the BM, the concordance with ctDNA detection was 100%, as all were ctDNA-negative. For patients with detectable bone marrow MRD, (8 of 29) 28% were ctDNA-positive, resulting in a NPV of 69%.

PRD-NGS and BM-MRD by NGF in the context of clinical disease progression

Table 2 presents the PPV, NPV, Se, and Sp of the different methods for measuring BM-MRD by NGF and PRD-NGS, and their association with disease progression. Among patients with positive results, disease progression occurred in 10 out of 39 BM-MRD-positive patients and in 8 out of 9 PRD-NGS-positive patients. Conversely, among patients with negative results, progression was not observed in 45 out of 47 BM-MRD-negative patients and in 63 out of 68 PRD-NGS-negative patients. Our method demonstrated a Se of 61.5% (and a Sp of 98.4%), outperforming traditional BM-MRD methods in Sp, which were notably lower at 70.3%. While BM-MRD by NGF showed higher Se (83.3%), the superior Sp (mentioned above) and PPV of our approach (88.9% vs. 34.5%) suggested improved ability to predict clinical progression. The lower PPV of NGF reflected the detection of true residual disease that did not result in overt progression within the follow-up period. The NPV was similar for both methods. As is standard practice, we compared our method against BM-MRD by NGF as the gold standard, and this comparison also revealed high Sp and PPV for PRD detection by NGS (Additional File 8, Table S3).

ctDNA detection impact on outcomes, PFS

As previously outlined, among the 77 patients monitored for ctDNA during follow-up, 9 (12%) had detectable ctDNA at one or more time points. In our cohort, the detection of ctDNA during follow-up correlated with a higher risk of disease progression. Univariable standard analysis showed that the risk of relapse was significantly higher in patients with positive ctDNA results than those with negative ctDNA (HR: 9.42, 95% CI: 3.49–25.4, P < 0.001). The median follow-up of the series was 43 m. The median PFS was 14 months in the ctDNA-positive group, while the median PFS was not reached in the ctDNA-negative group. Conversely, ctDNA negativity was associated with a 90% reduction in the risk of progression and/or death (HR: 0.10, 95% CI: 0.04–0.28, P < 0.001) (Figure 2A). Notably, among patients with positive BM-MRD by NGF (29/77), positive ctDNA by PRD-NGS identified those patients who had a poor prognosis (HR: 3.20, 95% CI: 1.02, 10.1, P = 0.04), suggesting that ctDNA may refine risk stratification within this high-risk subgroup (Figure 2B). Finally, time from first cfDNA positivity to relapse (median, IQR) was 128.5 days (79.5–361.2).

To further characterize the prognostic impact of MRD dynamics over the course of treatment, we used time-dependent Cox proportional hazards models to evaluate the association between MRD status (in both BM and ctDNA) and the risk of relapse. In univariable analysis, ctDNA positivity was significantly associated with increased risk of progression (HR: 10.3, 95% CI: 3.31–32.1, P < 0.001). Bivariate analysis adjusted for ctDNA showed an independent association of quadruplets with higher PFS (HR, 0.14; 0.03, 0.73). In the final multivariable Cox model, only BM-MRD positivity (HR: 4.26, 95% CI: 1.28–14.1, P = 0.018) and ctDNA positivity (HR: 11.4, 95% CI: 3.04–42.5, P < 0.001) were significantly associated with an increased risk of relapse. These findings reinforce the complementary prognostic role of PB ctDNA in the dynamic monitoring of minimal residual disease. Moreover, detectable ctDNA remained an independent prognostic factor for shorter PFS, underscoring the clinical value of ctDNA analysis. No significant effect on PFS was observed for the remaining variables (Figure 3 and Table 3).

TABLE 2 Distribution of the clinical course based on MRD assessment in bone marrow MRD and plasma ctDNA levels across patients.

Paired patients (BM/ct-DNA) and clinical course status	PRD NGS	BM-MRD NGF
BM-MRD^{pos} or ctDNA^{pos} —progression	8	10
BM-MRD^{neg} or ctDNA^{neg} —not progression	63	45
BM-MRD^{neg} or cDNAt^{neg} —progression	5	2
BM-MRD^{pos} or ctDNA^{pos} —not progression	1	19
Total (patients)	**77**	**76**
Positive predictive value (PPV%)	88.9	34.5
Negative predictive value (NPV%)	92.6	95.7
Specificity (Sp%)	98.4	70.3
Sensitivity (Se%)	61.5	83.3

Note: Positive predictive value (PPV), probability that a patient with a positive test result actually has the disease; negative predictive value (NPV), probability that a patient with a negative test result actually does not have the disease; specificity (Sp), ability of the method to correctly identify negative cases; sensitivity (Se), ability of the method to correctly identify positive cases.

Abbreviations: BM-MRD^{neg}, MRD not detectable in the bone marrow; BM-MRD^{pos}, MRD detectable in the bone marrow; Neg, negative; NGF, next-generation flow; NGS, next-generation sequencing; Pos, positive; PRD, peripheral residual disease.

DISCUSSION

Our study comprehensively evaluated cfDNA methodologies and their clinical impact on ctDNA detection for monitoring PRD-NGS in patients with MM. Our findings provide critical insights into the importance of initial plasma volume, the use of semi-automatic methodologies, and the clinical significance of ctDNA dynamics in disease monitoring. Notably, we observed an association between ctDNA detection and subsequent relapse.

Analysis of cfDNA levels across 292 plasma samples revealed a significant range in patients with MM, with extraction methods contributing to the observed variability and larger plasma volumes correlated with improved optimization of cfDNA recovery. In our integrity assessment, we noted that a significant proportion of cfDNA samples showed contamination with gDNA, particularly those isolated using the manual QCNA methodology, highlighting the need for purification steps to enhance the cfDNA quality for downstream applications and semi-automatic purification methods if specific tubes for cfDNA preservation are not used.

Plasma cfDNA levels remain stable for 24 h when whole blood is stored at 4°C in EDTA tubes without preservatives agents.[23,24] Although a high cfDNA yield was achieved, future studies may further improve cfDNA recovery by using specialized blood collection tubes that contain cell-stabilizing agents and nuclease inhibitors, such as Streck Cell-Free DNA BCT® tubes (La Vista, NE).

Encouragingly, our dual size-selection purification approach successfully removed gDNA in 98% of these samples, demonstrating its efficacy in improving cfDNA purity and enabling reliable detection of PRD-associated mutations. Automated methods achieved comparable cfDNA levels to manual methods, offering the advantages of standardization and high throughput.[25,26]

Overall, our preanalytical results suggest that the differences in cfDNA characteristics observed are partly attributable to cfDNA isolation techniques and initial plasma volume.

Therefore, standardized liquid biopsy workflows are favorable for accurate quantification and sensitive detection of cfDNA to avoid technical divergence at the pre-analytical stage and reduce its impact on downstream applications, such as biomarker testing or tumor mutation tracking for PRD-NGS monitoring.

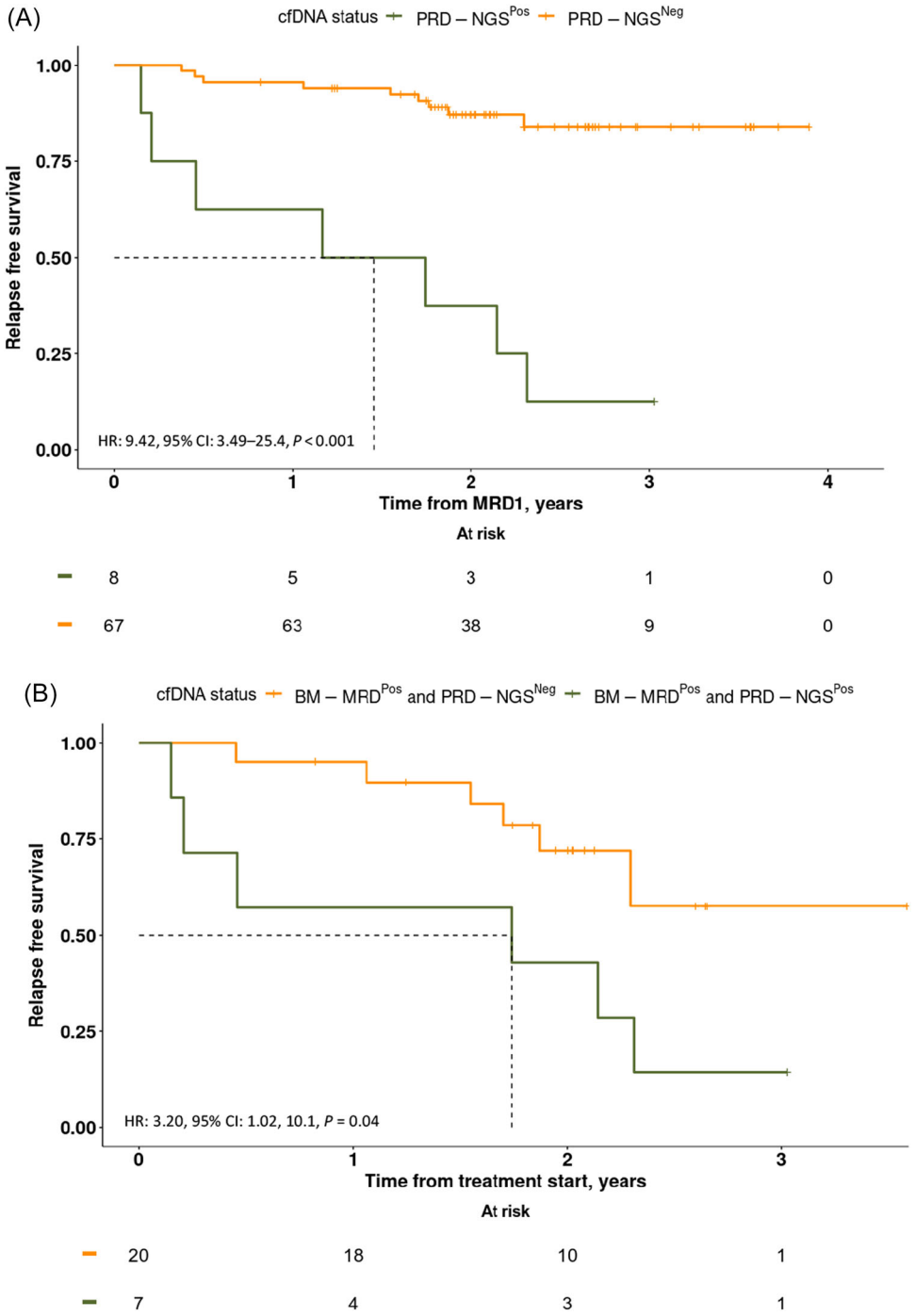

FIGURE 2 **Kaplan–Meier analysis of progression-free survival based on PRD monitoring by ctDNA detection. (A)** Impact of ctDNA detection using PRD-NGS on patient risk. Of the initial 77 patients, 75 were included in the final analysis; 2 were excluded due to disease progression prior to the first MRD assessment (MRD1). **(B)** Detectable ctDNA by AltumTrackSeq® predicts poorer prognosis in patients with BM-MRD positivity. BM-MRD, bone marrow measurable residual disease; NGS, next-generation sequencing; PRD, peripheral residual disease.

In this project, we have developed a highly sensitive method for ctDNA monitoring (AltumTrackSeq®). While current methods often analyze ~10 ng of DNA (~3000 hGE), our use of large plasma volumes and an input greater than 30 ng of cfDNA equivalent to ~10,000 hGE, patient-specific mutation panels, and the use of optimized tandem variants strategies enabled robust detection of low-frequency variants, thus achieving high Se. The number of informative reads generated and, thus the Se, is proportional to the input DNA (hGE) and the number of patient-specific mutations (selected biomarkers).[27] Consequently, increasing the initial DNA mass proportionally improves analytical Se, even in patients with limited detectable mutations at follow-up. Typical LoDs for current ctDNA assays range from 0.008% to 0.25% (or 80 to 2500 PPM).[28] Lower LoDs indicate higher Se and earlier detection of residual or recurrent disease. In our study, ctDNA concentrations in

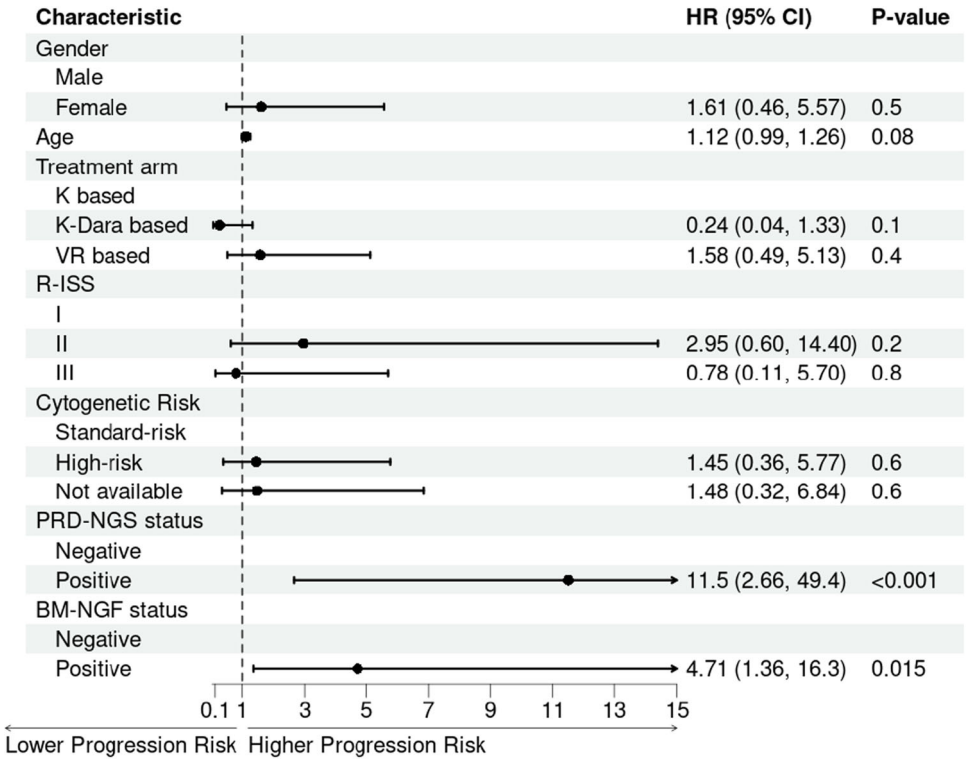

FIGURE 3 **Forest plot from multivariable Cox regression analysis examining factors associated with disease progression risk**. For each covariate, the hazard ratio (HR) and 95% confidence interval (CI) are presented. An HR < 1 signifies a lower risk of disease progression, whereas an HR > 1 signifies a higher risk. Statistically significant variables are highlighted by P < 0.05. PRD-NGS status (HR: 11.5, P < 0.001) and BM-NGF status (HR: 4.71, P = 0.015) were found to be both associated with a lower risk of progression. NGS, next-generation sequencing; PRD, peripheral residual disease.

TABLE 3 Univariate and multivariate time-dependent Cox analyses of PRD-NGS and BM-NFG at MRD1 for progression-free survival.

	Univariate Cox model (*n* = 75 patients)			Multivariate Cox model (*n* = 227 samples)[a]		
	HR	95% CI	P-value	HR	95% CI	P-value
Gender						
Male	—	—				
Female	0.99	0.37, 2.67	>0.9			
Age	1.08	0.97, 1.20	0.14	1.06	0.96, 1.17	0.2
Treatment arm						
Triplets	—	—		—	—	
Quadruplets	0.28	0.06, 1.25	0.10	0.25	0.05, 1.25	0.09
R-ISS						
I	—	—				
II	1.66	0.46, 6.00	0.4			
III	1.41	0.24, 8.49	0.7			
Cytogenetic risk						
Standard risk	—	—				
High risk	1.41	0.42, 4.69	0.6			
Not available	1.58	0.47, 5.26	0.5			
cfDNA status[b]	10.3	3.31, 32.1	**<0.001**	11.4	3.04, 42.5	**<0.001**
BM status[b]	6.70	2.15, 20.8	**0.001**	4.26	1.28, 14.1	**0.018**

Note: Treatment arms were grouped according to regimen intensity: triplet regimens included carfilzomib- or bortezomib-based combinations (K-based + VR-based), while quadruplet regimens included carfilzomib–daratumumab combinations (K-Dara-based).

Abbreviations: CI, confidence interval; HR, hazard ratio; R-ISS, Revised International Staging System.

[a]From the original 292 samples, those with DNA input below 30 ng or associated with early relapse before the first MRD assessment (MRD1) were excluded.

[b]The analysis was adjusted within the subset of positive versus negative patients. Statistically significant P-values (P < 0.05) are shown in bold in all analyses performed.

positive patients ranged from 125 to 8466 PPM, demonstrating a wide dynamic detection range. Furthermore, incorporation of tandem SNV mutations also enhanced Se by one to two additional orders of magnitude in the two patients tested in this study. Other advantages of this approach include scalability and standardization, consistent with similar technologies.[11,12] Using this approach, we achieved a theoretical Se of 10^{-5} in a high proportion of samples, and approximately 20% reached 10^{-6} (those with >350 ng of cfDNA and/or tandem mutations).

While ctDNA detection has proven useful for evaluating MRD in various solid tumors,[29–31] its role in MM is still emerging. However, ctDNA analyses hold promise as complementary tools to facilitate interim monitoring between invasive bone marrow evaluations.[32–36] The high PPV of PRD-NGS test suggests that identifying these events in positive patients could stratify those at imminent relapse risk. Early biochemical or clinical relapses following initial MRD positivity have been described and are not uncommon, as previously reported (Lasa M et al. Blood. 2025;146(8):964-970 and Blood Adv. 2022 Jan 31;6(3):808–817). Moreover, the superior Sp allowed for multimodality identification of MRD-negative patients with very low relapse risk, reducing false positives and improving clinical prediction, although it could be less useful in this situation. Conversely, a limitation of this study was that the Se for detecting plasma-positive cases was not superior to BM assessment according to our analysis. These findings likely relate to the significantly lower tumor burden in the PB of patients with MM.[37] They could also be related to the restricted number of BM-MRD-positive cases assessed by NGF and collected in our cohort, which should be considered in future studies. Nevertheless, the objective of PRD monitoring is to complement bone marrow evaluation without a substantial compromise in Se, especially when performed more frequently, and this has been successfully achieved.

Numerous studies have shown that MRD negativity reduces the risk of progression and mortality.[2,38] Our data support these findings, showing that patients with positive PRD detected by NGS had significantly less favorable PFS. Thus, ctDNA-PRD assessment by AltumTrackSeq® emerges as a good prognostic biomarker for PFS in patients with MM when compared with BM-MRD by NGF.

The main limitations of this study are its retrospective design and limited sample size, coupled with the lack of a direct comparison to NGS-based bone marrow MRD assessment using immunoglobulin genes. Further studies involving larger cohorts are actively being conducted to validate and expand these findings. Our group's prior comparative evaluations of CTCs, EM, and ctDNA further corroborate the concordant trends identified in this study.[5] Based on these results, detection of ctDNA with this highly sensitive method could serve as an alternative to minimize the need for invasive BM studies and facilitate more frequent monitoring of measurable residual disease through PB analysis, particularly in patients with MRD-positive BM findings. A further limitation concerns the relatively short median follow-up of 43 months, which raises the possibility that late events may have been missed. However, this follow-up period is in line with those reported in other similar studies.[39]

In summary, we have developed a highly sensitive technology for monitoring ctDNA in patients with MM, achieving an unprecedented Se of up to 10^{-6}. Our technology demonstrates high Sp and PPV, improving upon the detection of MRD in BM. Consequently, it offers a high-Se approach to assess PRD, providing a reliable tool for identifying patients at imminent risk of relapse. However, further studies will validate these findings.

ACKNOWLEDGMENTS

We are grateful to all researchers of *Grupo Español de Mieloma* (GEM) without whose dedication this study would not have come to fruition.

AUTHOR CONTRIBUTIONS

Natalia Buenache: Conceptualization; investigation; writing—original draft; methodology; validation; visualization; writing—review and editing; formal analysis. **Marta Lasa**: Writing—review and editing; data curation; resources. **Andrés Arroyo**: Conceptualization; writing—original draft; methodology; writing—review and editing; formal analysis; data curation. **Carmen González**: Writing—review and editing; resources. **Larissa Haertle**: Writing—review and editing. **Yanira Ruiz-Heredia**: Writing—review and editing. **Rosa Ayala**: Conceptualization; writing—review and editing; methodology. **Rafael Alonso**: Writing—review and editing. **Alejandro Martín-Muñoz**: Writing—review and editing; software; formal analysis. **Juan M. Rosa-Rosa**: Writing—review and editing. **Verónica González**: Writing—review and editing. **María J. Calasanz**: Writing—review and editing; resources; data curation. **Paula Rodríguez-Otero**: Writing—review and editing. **Laura Rosiñol**: Writing—review and editing. **Felipe De Arriba**: Writing—review and editing. **Enrique M. Ocio**: Writing—review and editing. **Albert Oriol**: Writing—review and editing. **Yolanda González**: Writing—review and editing. **Anna Sureda**: Writing—review and editing. **Sunil Lakhwani**: Writing—review and editing. **María E. Clavero**: Writing—review and editing. **Angela Ibáñez**: Writing—review and editing. **Clara Gómez**: Writing—review and editing. **Alberto Orfao**: Writing—review and editing. **María-Victoria Mateos**: Writing—review and editing. **Juan J. Lahuerta**: Writing—review and editing. **María T. Cedena**: Writing—review and editing; conceptualization. **Joan Bladé**: Writing—review and editing. **Jesús San Miguel**: Writing—review and editing. **Noemi Puig**: Writing—review and editing. **Bruno Paiva**: Conceptualization; investigation; writing—review and editing; supervision. **Joaquín Martínez-López**: Conceptualization; investigation; funding acquisition; writing—original draft; methodology; validation; visualization; writing—review and editing; data curation; supervision; resources; project administration.

CONFLICT OF INTEREST STATEMENT

VGC discloses consulting or advisory role: Johnson & Johnson and GlaxoSmithKline. Speakers' bureau: Johnson & Johnson, GlaxoSmithKline, and Pfizer. Travel, accommodations, expenses: Johnson & Johnson, GlaxoSmithKline, and Pfizer. FdA declares honoraria derived from lectures and participation in advisory boards: Johnson&Johnson, Celgene-BMS, Amgen, GSK, Sanofi, Menarini, Oncopeptides, Pfizer, and Takeda. EMO discloses honoraria/consulting fees from AbbVie, Amgen, AstraZeneca, BMS, GSK, Janssen, Menarini, Oncopeptides, Pfizer, Regeneron, Sanofi, and Takeda. BP reports consultancy fees from BMS-Celgene, GSK, Janssen, Roche, Sanofi, and Takeda; research funding from AstraZeneca, BeiGene, BMS, GSK, Roche, and Sanofi; and honoraria from Adaptive, Amgen, Becton/Dickinson Biosciences, BMS-Celgene, GSK, Janssen, Roche, and Sanofi. JML is an advisor for BMS, Pfizer, Amgen, Roche, Novartis, J&J, and Incyte, and has shares in Altum sequencing and Statb therapeutics. JML also received grants support from BMS, Pfizer, and Amgen.

DATA AVAILABILITY STATEMENT

Data are provided within the manuscript or supplementary information files.

The data that support the findings of this study are openly available in NIH at https://www.ncbi.nlm.nih.gov/sra/PRJNA1280803, reference number PRJNA1280803.

ETHICS STATEMENT

This study was performed in accordance with the Declaration of Helsinki and in compliance with good clinical practice guidelines and applicable laws. The protocol was approved by the institutional review boards or ethics committee at study sites. Written informed

consent was obtained before study entry from each patient or from the patient's legally authorized representative if the patient was unable to provide consent.

FUNDING

This study was supported by the *CRIS Contra el Cáncer Foundation* (2021/0088 and 2024/0031) and the *Fondo de Investigación Sanitaria* (FIS; PI21/01751).

SUPPORTING INFORMATION

Additional supporting information can be found in the online version of this article.

ORCID

Natalia Buenache https://orcid.org/0009-0009-9145-3462
Carmen González https://orcid.org/0009-0001-3074-9229
Larissa Haertle https://orcid.org/0000-0002-3927-9163
Rafael Alonso https://orcid.org/0000-0003-3774-118X
Paula Rodríguez-Otero https://orcid.org/0000-0001-5236-7785
Felipe De Arriba https://orcid.org/0000-0002-4451-1318
Sunil Lakhwani https://orcid.org/0000-0003-1984-4839
Alberto Orfao https://orcid.org/0000-0002-0007-7230
Noemi Puig https://orcid.org/0000-0001-7535-3861
Bruno Paiva https://orcid.org/0000-0003-1977-3815

REFERENCES

1. Martinez-Lopez J, Lahuerta JJ, Pepin F, et al. Prognostic value of deep sequencing method for minimal residual disease detection in multiple myeloma. *Blood*. 2014;123(20):3073-3079. doi:10.1182/blood-2014-01-550020
2. Munshi NC, Avet-Loiseau H, Rawstron AC, et al. Association of minimal residual disease with superior survival outcomes in patients with multiple myeloma: a meta-analysis. *JAMA Oncology*. 2017;3(1):28-35. doi:10.1001/jamaoncol.2016.3160
3. Paiva B, Puig N, Cedena MT, et al. Measurable residual disease by next-generation flow cytometry in multiple myeloma. *J Clin Oncol*. 2020;38(8):784-792. doi:10.1200/JCO.19.01231
4. Alonso R, Cedena MT, Gómez-Grande A, et al. Imaging and bone marrow assessments improve minimal residual disease prediction in multiple myeloma. *Am J Hematol*. 2019;94(8):853-861. doi:10.1002/ajh.25507
5. Lasa M, Notarfranchi L, Agullo C, et al. Minimally invasive assessment of peripheral residual disease during maintenance or observation in transplant-eligible patients with multiple myeloma. *J Clin Oncol*. 2025;43(2):125-132. doi:10.1200/JCO.24.00635
6. Leon SA, Shapiro B, Sklaroff DM, Yaros MJ. Free DNA in the serum of cancer patients and the effect of therapy. *Cancer Res*. 1977;37(3):646-650.
7. Stroun M, Anker P, Maurice P, Lyautey J, Lederrey C, Beljanski M. Neoplastic characteristics of the DNA found in the plasma of cancer patients. *Oncology*. 1989;46(5):318-322. doi:10.1159/000226740
8. Cohen JD, Li L, Wang Y, et al. Detection and localization of surgically resectable cancers with a multi-analyte blood test. *Science*. 2018;359(6378):926-930. doi:10.1126/science.aar3247
9. Poulet G, Massias J, Taly V. Liquid biopsy: general concepts. *Acta Cytol*. 2019;63(6):449-455. doi:10.1159/000499337
10. Song P, Wu LR, Yan YH, et al. Limitations and opportunities of technologies for the analysis of cell-free DNA in cancer diagnostics. *Nat Biomed Eng*. 2022;6(3):232-245. doi:10.1038/s41551-021-00837-3
11. Kurtz DM, Soo J, Co Ting Keh L, et al. Enhanced detection of minimal residual disease by targeted sequencing of phased variants in circulating tumor DNA. *Nat Biotechnol*. 2021;39(12):1537-1547. doi:10.1038/s41587-021-00981-w
12. Foltz SM, Li Y, Yao L, et al. Somatic mutation phasing and haplotype extension using linked-reads in multiple myeloma. *bioRxiv* [Preprint]. 2024. doi:10.1101/2024.08.09.607342
13. Jiménez-Ubieto A, Poza M, Martin-Muñoz A, et al. Real-life disease monitoring in follicular lymphoma patients using liquid biopsy ultra-deep sequencing and PET/CT. *Leukemia*. 2023;37(3):659-669. doi:10.1038/s41375-022-01803-x
14. Jiménez-Ubieto A, Martín-Muñoz A, Poza M, et al. Personalized monitoring of circulating tumor DNA with a specific signature of trackable mutations after chimeric antigen receptor T-cell therapy in follicular lymphoma patients. *Front Immunol*. 2023;14:1188818. doi:10.3389/fimmu.2023.1188818
15. Chauhan PS, Chen K, Babbra RK, et al. Urine tumor DNA detection of minimal residual disease in muscle-invasive bladder cancer treated with curative-intent radical cystectomy: a cohort study. *PLoS Med*. 2021;18(8):e1003732. doi:10.1371/journal.pmed.1003732
16. Rosa-Rosa JM, Cuenca I, Medina A, et al. NGS-based molecular karyotyping of multiple myeloma: results from the GEM12 clinical trial. *Cancers*. 2022;14(20):5169. doi:10.3390/cancers14205169
17. Dang DK, Park BH. Circulating tumor DNA: current challenges for clinical utility. *J Clin Invest*. 2022;132(12):e154941. doi:10.1172/JCI154941
18. Onecha E, Linares M, Rapado I, et al. A novel deep targeted sequencing method for minimal residual disease monitoring in acute myeloid leukemia. *Haematologica*. 2019;104(2):288-296. doi:10.3324/haematol.2018.194712
19. Sánchez R, Dorado S, Ruíz-Heredia Y, et al. Author Correction: detection of kinase domain mutations in BCR::ABL1 leukemia by ultra-deep sequencing of genomic DNA. *Sci Rep*. 2024;14(1):7400. doi:10.1038/s41598-024-57570-5
20. Flores-Montero J, Sanoja-Flores L, Paiva B, et al. Next generation flow for highly sensitive and standardized detection of minimal residual disease in multiple myeloma. *Leukemia*. 2017;31(10):2094-2103. doi:10.1038/leu.2017.29
21. Lahuerta JJ, Paiva B, Vidriales MB, et al. Depth of response in multiple myeloma: a pooled analysis of three PETHEMA/GEM clinical trials. *J Clin Oncol*. 2017;35(25):2900-2910. doi:10.1200/JCO.2016.69.2517
22. Tabares-Gaviria P, Schmiedgen K, Dhanraj J, et al. Euroflow-based ultrasensitive NGF for the evaluation of bone marrow minimal residual disease in multiple myeloma. *Blood*. 2023;142(Suppl 1):3342.
23. Parpart-Li S, Bartlett B, Popoli M, et al. The effect of preservative and temperature on the analysis of circulating tumor DNA. *Clin Cancer Res*. 2017;23(10):2471-2477. doi:10.1158/1078-0432.CCR-16-1691
24. Meddeb R, Pisareva E, Thierry AR. Guidelines for the preanalytical conditions for analyzing circulating cell-free DNA. *Clin Chem*. 2019;65(5):623-633. doi:10.1373/clinchem.2018.298323
25. Pérez-Barrios C, Nieto-Alcolado I, Torrente M, et al. Comparison of methods for circulating cell-free DNA isolation using blood from cancer patients: impact on biomarker testing. *Transl Lung Cancer Res*. 2016;5(6):665-672. doi:10.21037/tlcr.2016.12.03
26. Bronkhorst AJ, Ungerer V, Holdenrieder S. Comparison of methods for the isolation of cell-free DNA from cell culture supernatant. *Tumor Biol*. 2020;42(4):1010428320916314. doi:10.1177/1010428320916314
27. Wan JCM, Heider K, Gale D, et al. ctDNA monitoring using patient-specific sequencing and integration of variant reads. *Sci Transl Med*. 2020;12(548):eaaz8084. doi:10.1126/scitranslmed.aaz8084
28. Northcott J, Bartha G, Harris J, et al. Correction: Analytical validation of NeXT Personal®, an ultra-sensitive personalized circulating tumor DNA assay. *Oncotarget*. 2024;15:407. doi:10.18632/oncotarget.28581

29. Pantel K, Alix-Panabières C. Liquid biopsy and minimal residual disease—latest advances and implications for cure. *Nat Rev Clin Oncol*. 2019;16(7):409-424. doi:10.1038/s41571-019-0187-3
30. Faulkner LG, Howells LM, Pepper C, Shaw JA, Thomas AL. The utility of ctDNA in detecting minimal residual disease following curative surgery in colorectal cancer: a systematic review and meta-analysis. *Br J Cancer*. 2023;128(2):297-309. doi:10.1038/s41416-022-02017-9
31. Zhu L, Xu R, Yang L, et al. Minimal residual disease (MRD) detection in solid tumors using circulating tumor DNA: a systematic review. *Front Genet*. 2023;14:1172108. doi:10.3389/fgene.2023.1172108
32. Medina-Herrera A, Sarasquete ME, Jiménez C, Puig N, García-Sanz R. Minimal residual disease in multiple myeloma: past, present, and future. *Cancers*. 2023;15(14):3687. doi:10.3390/cancers15143687
33. Manier S, Park J, Capelletti M, et al. Whole-exome sequencing of cell-free DNA and circulating tumor cells in multiple myeloma. *Nat Commun*. 2018;9(1):1691. doi:10.1038/s41467-018-04001-5
34. Gerber B, Manzoni M, Spina V, et al. Circulating tumor DNA as a liquid biopsy in plasma cell dyscrasias. *Haematologica*. 2018;103(6):e245-e248. doi:10.3324/haematol.2017.184358
35. Kis O, Kaedbey R, Chow S, et al. Circulating tumour DNA sequence analysis as an alternative to multiple myeloma bone marrow aspirates. *Nat Commun*. 2017;8:15086. doi:10.1038/ncomms15086
36. Kogure Y, Handa H, Ito Y, et al. ctDNA improves prognostic prediction for patients with relapsed/refractory MM receiving ixazomib, lenalidomide, and dexamethasone. *Blood*. 2024;143(23):2401-2413. doi:10.1182/blood.2023022540
37. Garcés JJ, Cedena MT, Puig N, et al. Circulating tumor cells for the staging of patients with newly diagnosed transplant-eligible multiple myeloma. *J Clin Oncol*. 2022;40(27):3151-3161. doi:10.1200/JCO.21.01365
38. Perrot A, Lauwers-Cances V, Corre J, et al. Minimal residual disease negativity using Deep sequencing is a major prognostic factor in multiple myeloma. *Blood*. 2018;132(23):2456-2464. doi:10.1182/blood-2018-06-858613
39. Mohan M, Kendrick S, Szabo A, et al. Clinical implications of loss of bone marrow minimal residual disease negativity in multiple myeloma. *Blood Adv*. 2022;6(3):808-817. doi:10.1182/bloodadvances.2021005822